Silver in geological fluids from in situ X-ray absorption spectroscopy and first-principles molecular dynamics

Pokrovski, Gleb S ; Roux, Jacques ; Ferlat, Guillaume ; Jonchiere, Romain ; Seitsonen, Ari P ; Vuilleumier, Rodolphe ; Hazemann, Jean-Louis

DOI: https://doi.org/10.1016/j.gca.2012.12.012

Supplementary Electronic Information

Electronic annex 1

Continuous Cauchy Wavelet Transform analysis of EXAFS spectra of selected Ag-chloride and nitrate solutions

Supplementary Figure EA-1. Continuous Cauchy Wavelet Transform analysis (CCWT, Munoz et al., 2003) of selected Ag K-edge EXAFS spectra of silver nitrate and silver chloride solutions at 600 bar and indicated temperature and composition, recorded in this study. Each graph represents k^2-weighted experimental spectrum, its Fourier Transform magnitude, and CCWT modulus showing the localization of each EXAFS contribution in (k, R) space. The color intensity is proportional to the magnitude of the CCWT modulus (blue to dark-blue = low, red to brown = high). The vertical lines indicate the maximum intensity positions for O and Cl neighbors around the Ag absorber. It can be seen in Fig. EA1-1A that these maximum intensity positions in both k- and R-space are distinctly different for O and Cl atoms around Ag, thus allowing clear identification of the presence of these backscatterrers in the experimental spectrum. In can be seen in Fig. EA1-1B and EA-1C that no oxygen contribution is detected in all studied Cl-bearing solutions in a wide T (200-450°C) and total Cl concentration range (0.7-6.0 mol/kg), and that the signal is dominated by Cl backscatterrers. Note, that with increasing Cl content (e.g., Fig. EA1-1B) and decreasing temperature (Fig. 1C), the shape of CCW Transform becomes wider and less symmetrical, indicating larger disorder in the Ag-Cl distances at high m_{Cl} and low T. This is in agreement with quantitative EXAFS fits showing the increase of DW factors and anharmonic cumulant c_3 parameter (Table 1). This is in line with the presence of different silver chloride complexes at low T and high chlorinity as suggested by available solubility studies (Seward, 1976).

References for Electronic annex 1

Munoz, M., Argoul, P., Farges F., 2003. Continuous cauchy wavelet transform analyses of EXAFS spectra: a qualitative approach. Amer. Mineral. 88, 694-700.

Seward T.M. (1976) The stability of chloride complexes of silver in hydrothermal solutions up to 350°C. Geochim. Cosmochim. Acta 40, 1329-1341.

exp #1, 0.21m $AgNO_3$-0.10m HNO_3-0.10m H_2O_2, 30°C

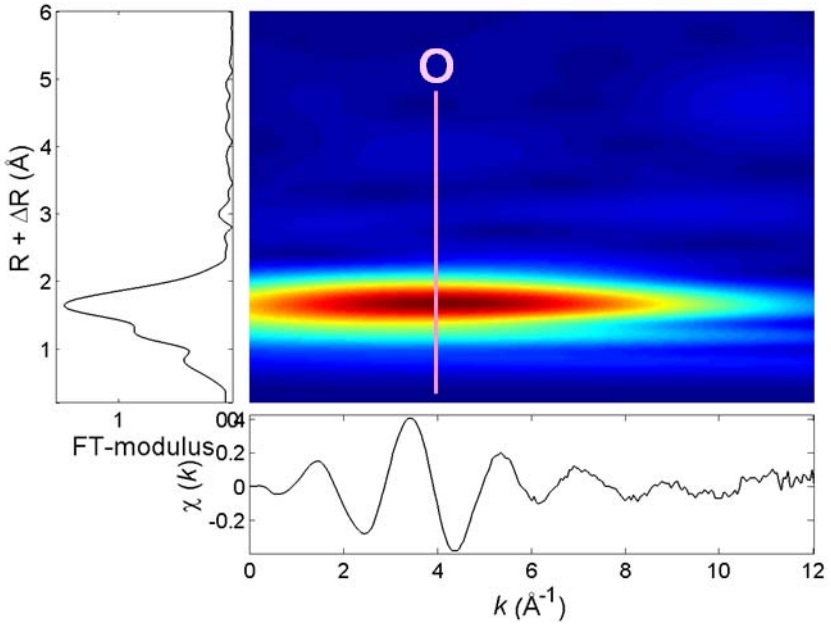

exp #4, 0.18m AgCl-2.34m NaCl-0.12m HCl-0.10m H_2O_2, 200°C

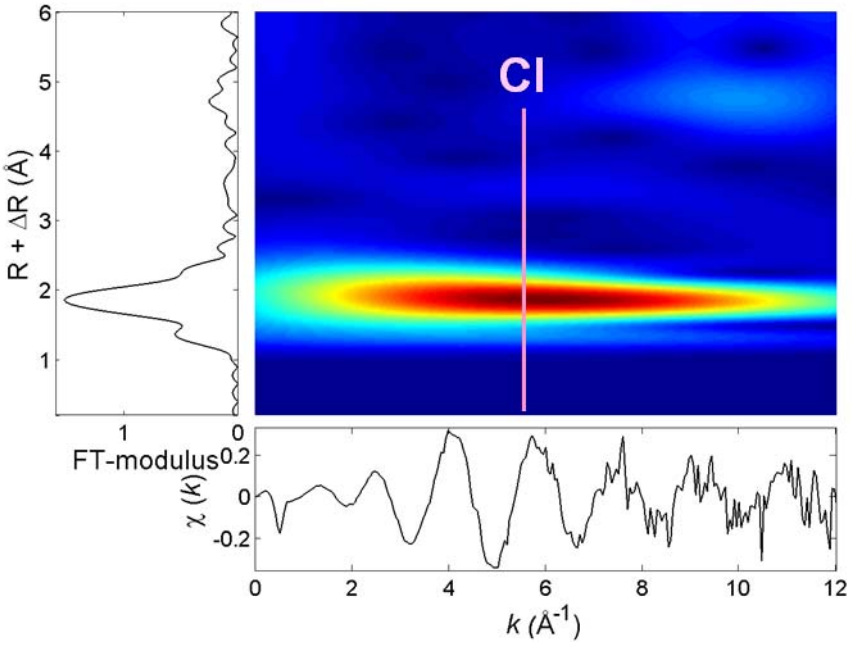

Fig. EA1-1A

exp #6, 0.17m AgCl-0.42m NaCl-0.11m HCl-0.06m H_2O_2, 400°C

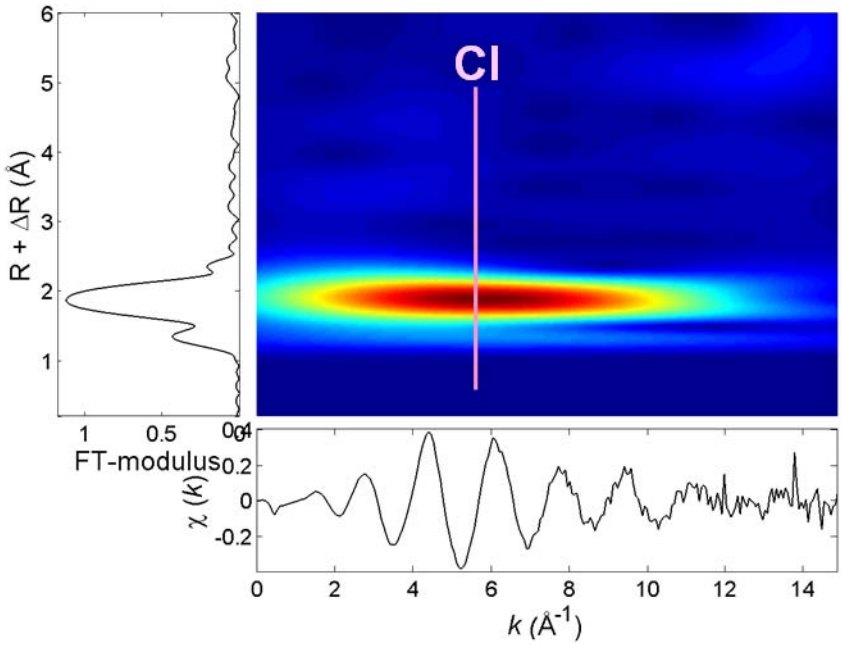

exp #4, 0.18m AgCl-2.34m NaCl-0.12m HCl-0.06m H_2O_2, 400°C

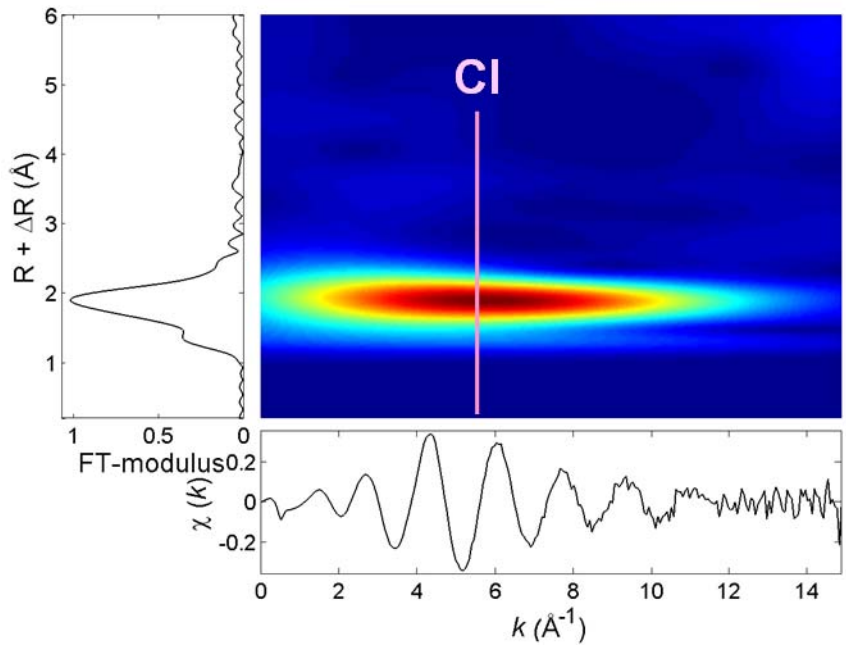

Fig. EA1-1B

exp #5, 0.30m AgCl-5.51m NaCl-0.14m HCl-0.07m H_2O_2, 200°C

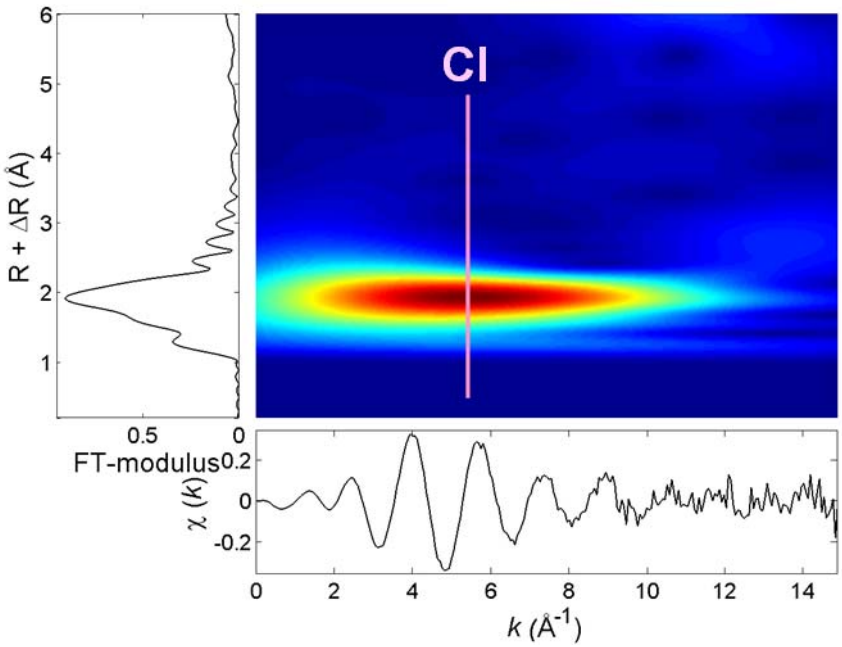

exp #5, 0.30m AgCl-5.51m NaCl-0.14m HCl-0.07m H_2O_2, 450°C

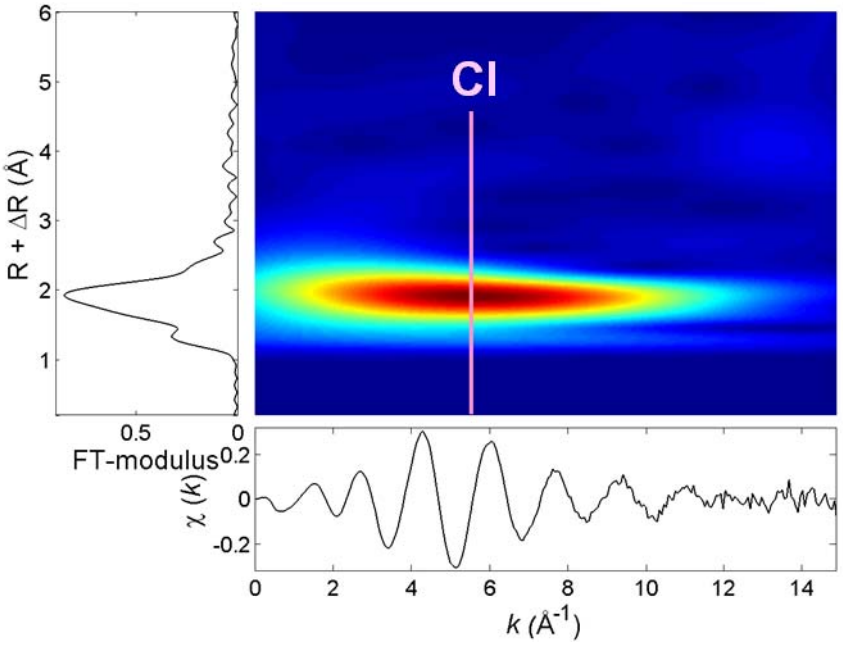

Fig. EA1-1C

Electronic annex 2

Examples of EXAFS fits of representative Ag-chloride and nitrate solutions

Supplementary Figure EA2-1. EXAFS fits in chi(k)×k^2-space and R-space (both FT magnitude and imaginary part) of (A) 0.21*m* $AgNO_3$-0.1*m* HNO_3-0.10*m* H_2O_2 solution (exp #1, 0*m* total Cl) at 200°C/600bar, (B) 0.17*m* AgCl-0.42*m* NaCl-0.11*m* HCl-0.06*m* H_2O_2 solution (exp #6, 0.70m total Cl) at 450°C/700 bar, and (C) 0.30*m* AgCl-5.51*m* NaCl-0.14*m* HCl-0.07*m* H_2O_2 solution (exp #5, 5.9m total Cl) at 300°C/600 bar. For all samples the fitted R-ranges are 1.1-2.8 Å (not corrected for phase shift), and k-ranges are 2.5-10.0 $Å^{-1}$ and 3.0-11.8 $Å^{-1}$ for nitrate and chloride solutions, respectively. Blue curves = experimental spectrum, red curves = fit.

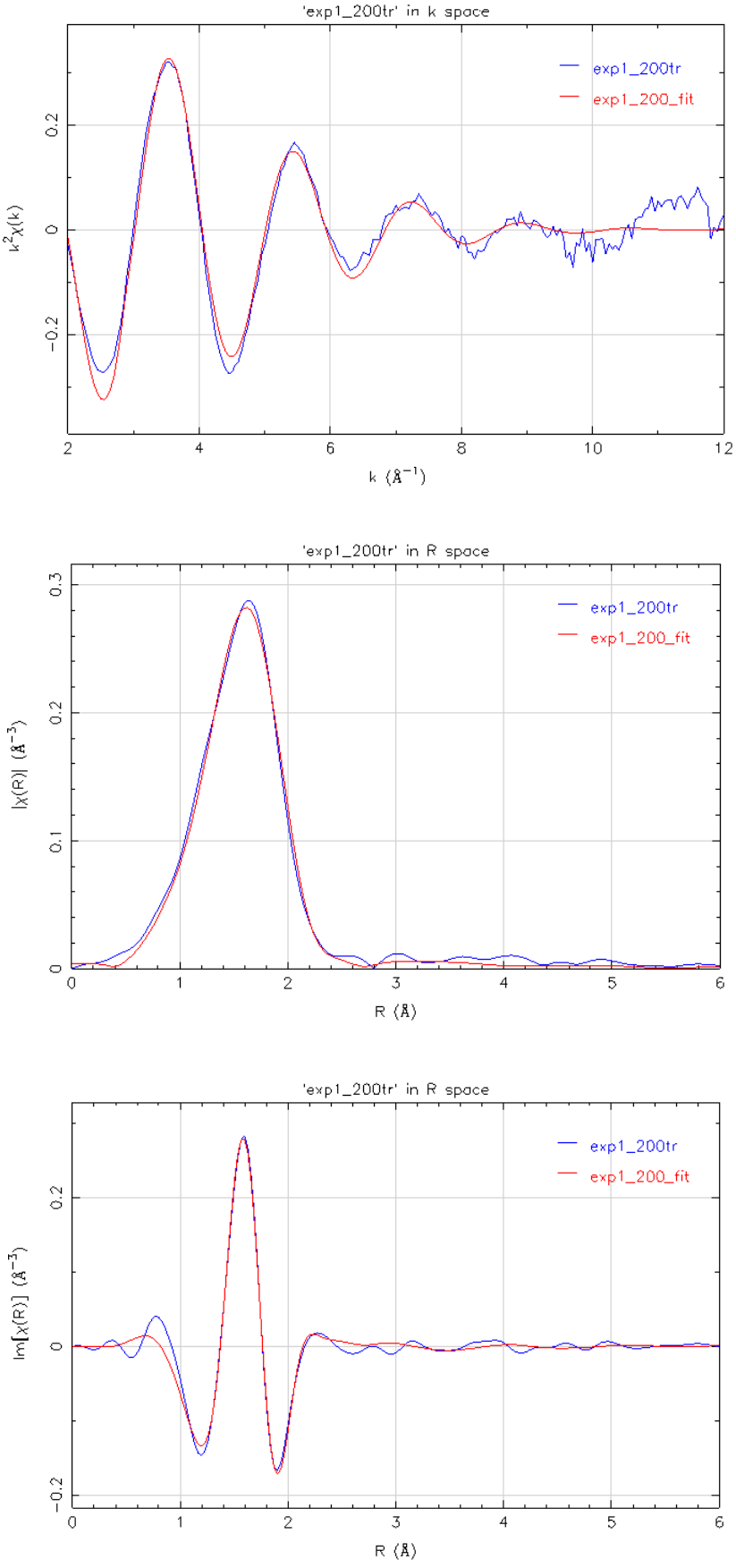

Fig. EA2-1A, exp #1, 0*m* Cl_{tot}, 200°C/600 bar

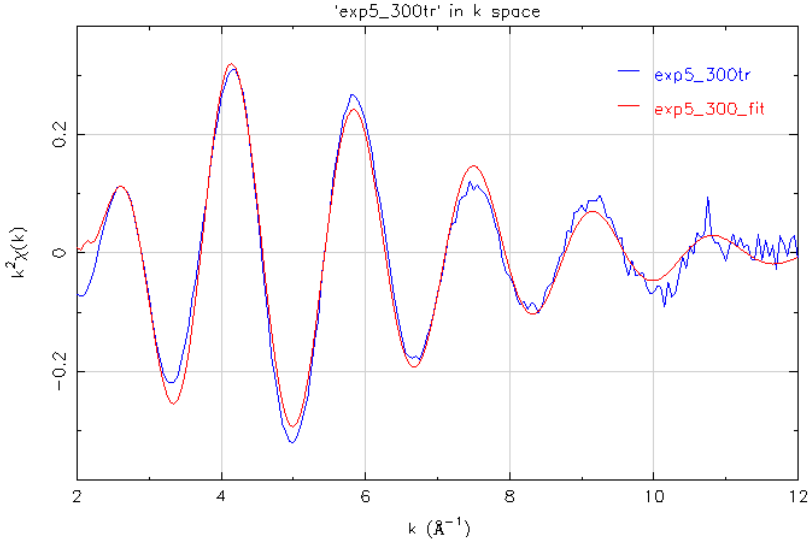

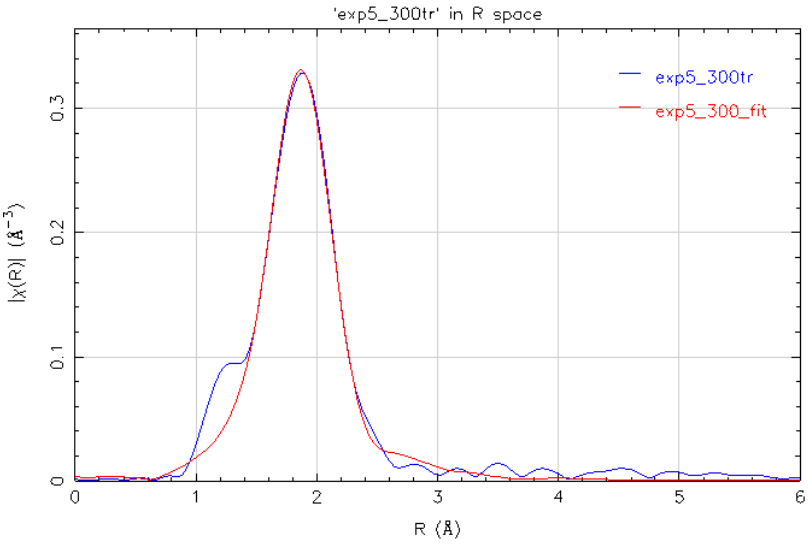

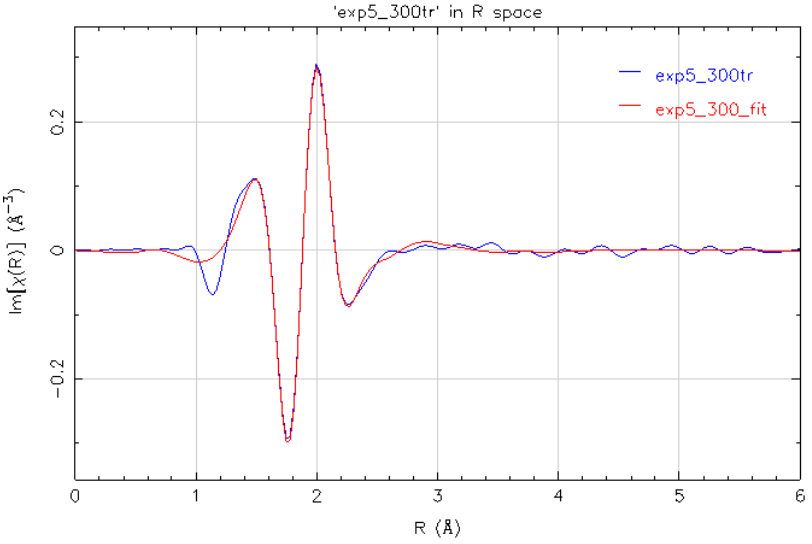

Fig. EA2-1B, exp #6, 0.70*m* Cl_{tot}, 450°C/700 bar

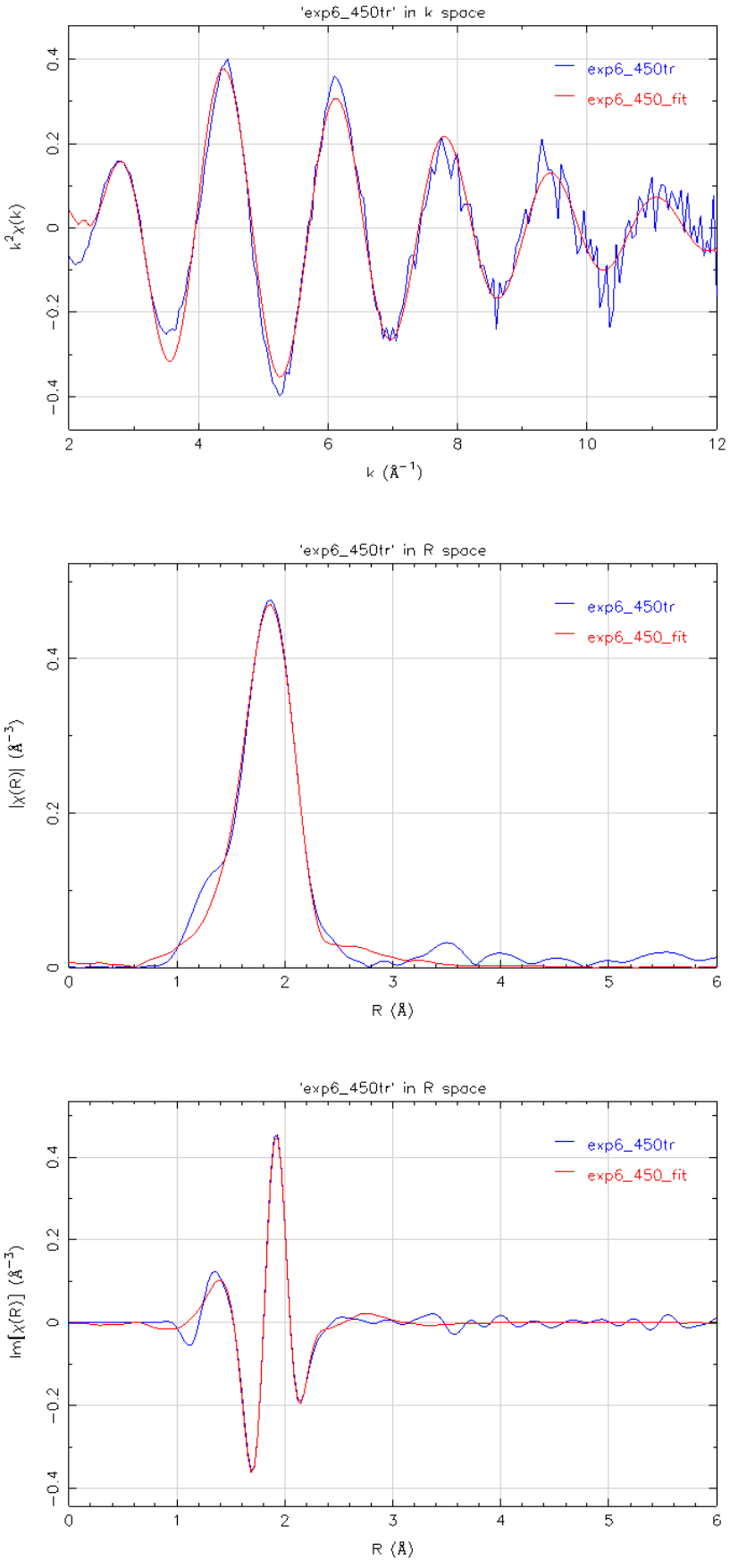

Fig. EA2-1C, exp #5, 5.9*m* Cl_{tot}, 300°C/600 bar

Electronic annex 3

Calculated XANES spectra for Ag-bearing solid phases and Ag-O model clusters, and their comparison with experimental data

Supplementary Figure EA3-1. Comparison of XANES spectra for silver nitrate and silver chloride solid phases calculated using the FDMNES program and measured in this study.

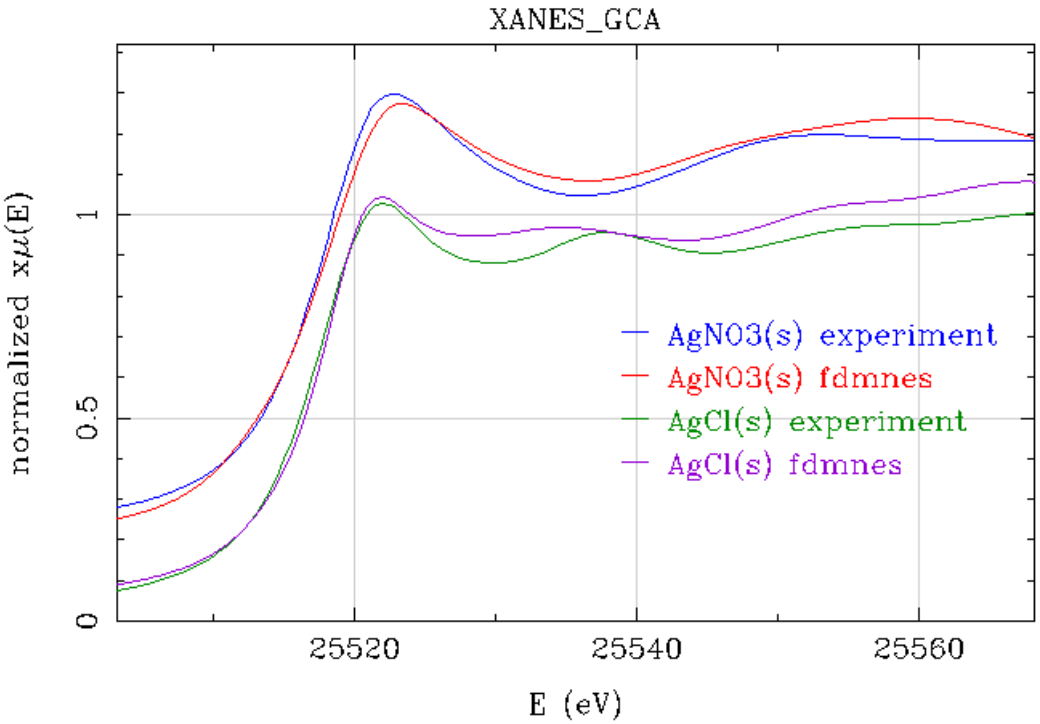

Supplementary Figure EA3-2. Comparison of experimental XANES spectra from the Ag-bearing nitrate solution with calculated XANES spectra for representative Ag-O clusters of different geometry and stoichiometry.

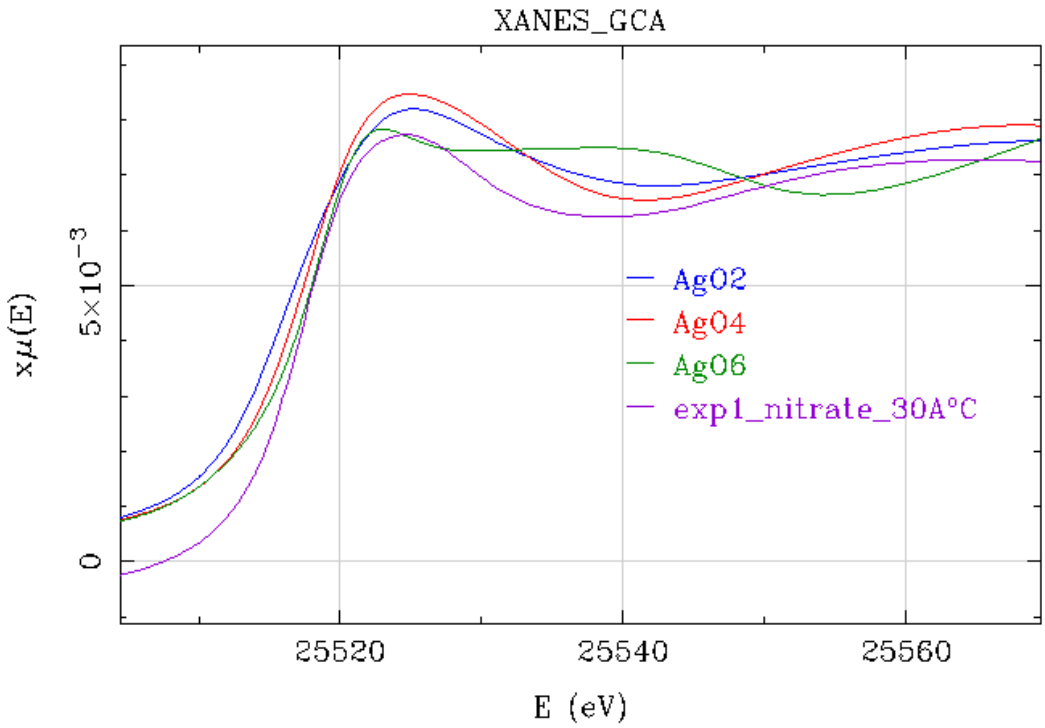

Electronic annex 4

Ag-Cl distances as a function of simulation time calculated by molecular dynamics

Supplementary Figure EA4-1. Ag-Cl distances as a function of the simulation time (in picosecond) at 50°C calculated for the system containing one Ag^+, 4 Cl^-, and 1 Na^+. The vertical dotted lines separate regions of time where different types of complexes are identified: I) $AgCl_4^{3-}$ II) $AgCl_3^{2-}$ III) $AgCl_3(H_2O)^{2-}$ IV) $AgCl_2^-$.

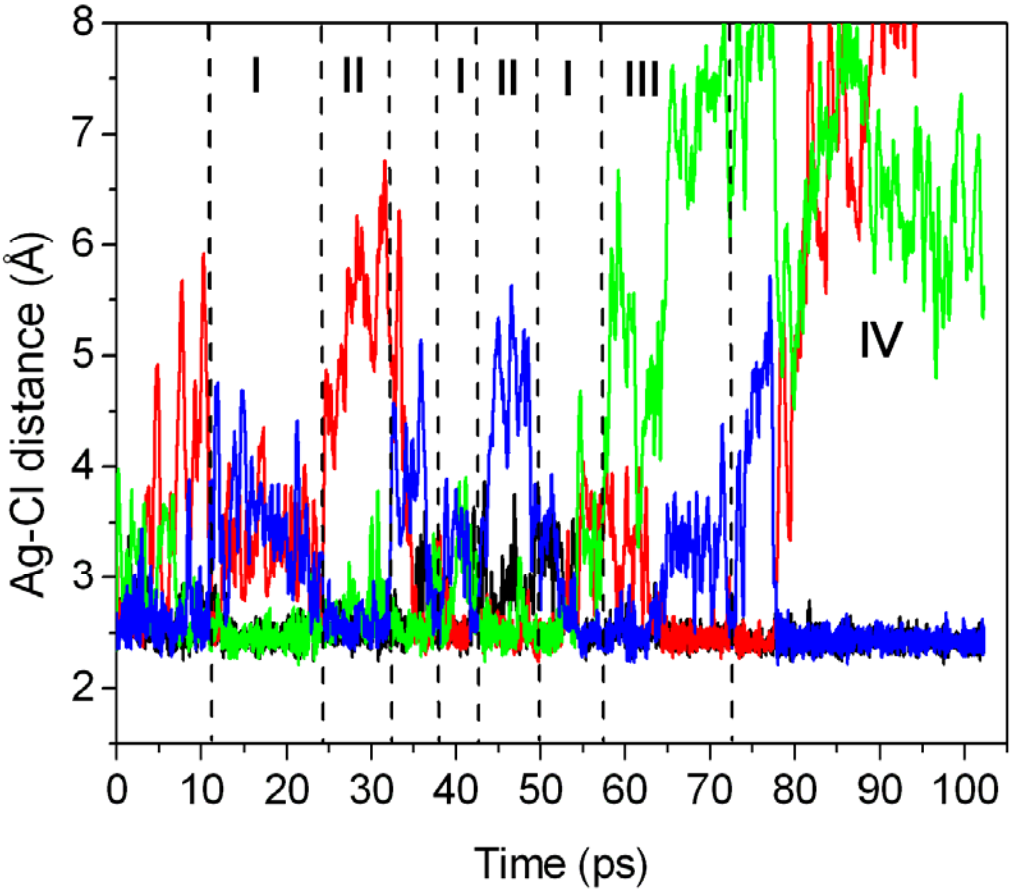

Supplementary Figure EA4-2. Ag-Cl distances as a function of the simulation time (in picosecond) at 380°C in the system containing 1 Ag^+, 2 Cl^-, and 1 Na^+. The vertical dotted lines separate regions of time where different types of complexes are identified: I) $AgCl(H_2O)$, II) $AgCl_2^-$.

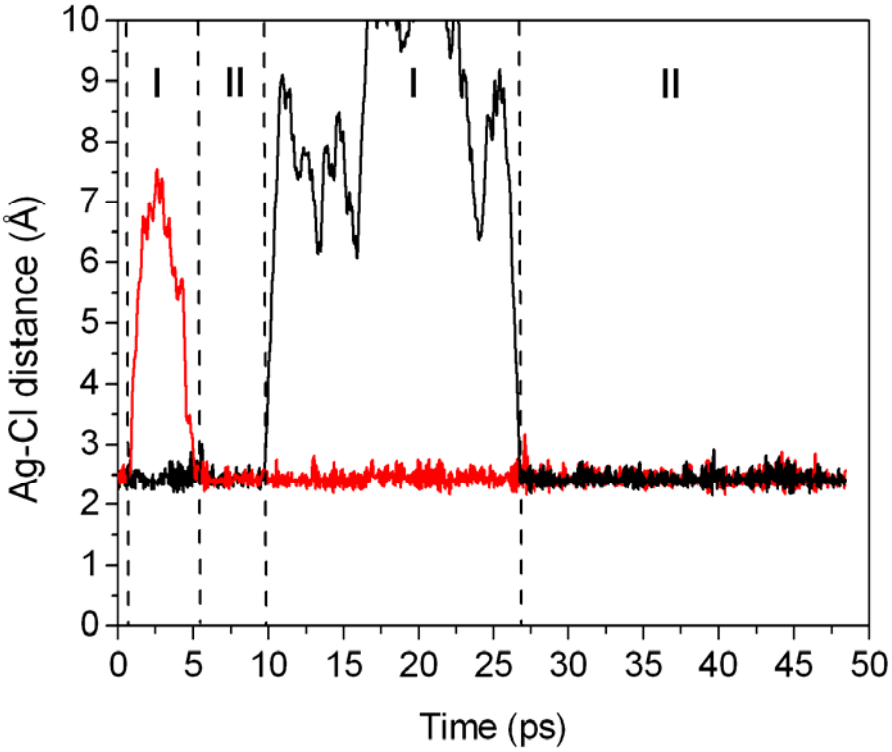

Supplementary Figure EA4-3. Ag-Na radial distribution functions (a) in the system Na-Ag-4Cl at 50°C, 1 bar, and (b) in the system Na-AgCl2 at 380°C and 600 bar.